DOI: 10.1002/ejic.200800736

Langmuir–Schäfer Films of Functional Amphiphilic Nickel(II) and Zinc(II) Schiff Base Complexes

Santo Di Bella,*[a] Giuseppe Consiglio,[b] Salvatore Sortino,*[a] Gabriele Giancane,[c] and Ludovico Valli*[c]

Keywords: Multilayers / Fluorescence / Schiff bases / Nickel / Zinc

The synthesis of novel functional amphiphilic dipodal Ni^{II} (**1**) and Zn^{II} (**2**) Schiff base complexes and the preparation/characterization and optical properties of Langmuir–Schäfer (LS) multilayer films are reported. The existence of stacked 3D aggregates is observed for all films, as established by the combination of reflection spectroscopy and Brewster angle microscopy. Although aggregate formation does not involve major electronic changes, as evidenced by analysis by absorption spectroscopy, fluorescence emission is much more sensitive to the chemical environment, and complete quenching is observed in the multilayer LS aggregates. However, in the limit of negligible interchromophore interactions, achieved by means of mixed LS multilayer films the fluorescence is restored by using arachidic acid as a spacer diluent, and LS layers of **2** behave as related self-assembled monolayers.

Introduction

The molecular organization in defined assemblies is one of the most interesting issues in the growing field of molecular electronics and optoelectronics.[1,2] In this regard, the Langmuir–Blodgett (LB) technique represents a powerful tool to tailor and develop functional molecular assemblies of defined structures.[3] Various classes of molecular materials have been studied as LB films, ranging from simple functional organic molecules[3] to complex functional systems.[4]

Recently, metal Schiff base complexes have been investigated for their diverse properties.[5–7] The role of the metal centre in determining the characteristics of these complexes is manifold. It has been shown that the catalytic,[5] fluorescent,[6] and nonlinear optical properties[7] and their possible interplay with magnetic coupling[7c] of these complexes are strictly related to the coordinated metal.

LB films of Schiff bases have previously been prepared, and the related structure investigated. In particular, mono- and multilayers of alkyl-substituted Schiff bases and related complexes,[8] some formed at the water/air interface,[9] have been examined. In all cases, however, either in the presence of short alkyl or long *N*-alkyl-substituted side chains, these species lead to the formation of aggregates,[8,9] with structures in which the aromatic rings have a nearly flat orientation with respect to the water surface or the substrate.[8,9] The horizontal lifting method [Langmuir–Schäfer (LS) technique] has also been used in order to deposit films of both unsubstituted and substituted Schiff bases.[10] Interestingly, it was found that chiral supramolecular assemblies were obtained from achiral Schiff bases with or without alkyl chains, probably because of stereoregular π–π stacking.[10]

The presence of dipodal alkyl side chains in the salicylidene rings of the Schiff base offers an interesting possibility of investigating its adopted structure and properties in the formation of multilayer LB films. Molecules with large head groups and the long alkyl derivatization have been used for the construction of LB films. The design of moieties with such a cross-sectional mismatch between the alkyl tail and the head group has been of great interest not only in the case of Schiff bases,[9a] but also for other important functional molecules such as merocyanines.[11] In this paper, we report on the synthesis of novel functional[6,7] amphiphilic Ni^{II} and Zn^{II} Schiff base complexes (Scheme 1) and the preparation/characterization and optical properties of LS multilayer films. Studies on the photoprocesses involving thin films and their modulation through changes in the molecular environment of active materials are a subject of thorough investigations. In our case, fluorescence emission has been activated, depending on the molecular organization of the active species inside the LS films.

[a] Dipartimento di Scienze Chimiche, Università di Catania, 95125 Catania, Italy
E-mail: sdibella@unict.it
ssortino@unict.it
[b] Dipartimento di Metodologie Fisiche e Chimiche per l'Ingegneria, Università di Catania, 95125 Catania, Italy
[c] Dipartimento di Ingegneria dell'Innovazione, Università degli Studi del Salento, 73100 Lecce, Italy
E-mail: ludovico.valli@unile.it

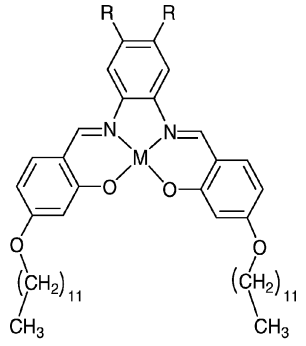

R = Cl; M = Ni **1**
R = H; M = Zn **2**

Scheme 1.

Results and Discussion

The dipodal alkyl-derivatized Schiff base complexes **1** and **2** were synthesized by a nucleophilic substitution reaction between the 4-hydroxy substituted bis(salicylaldiminato)Zn^{II} complex or the related Ni^{II} phenoxide disodium salt and 1-iodododecane. Amphiphilic complexes **1** and **2** are insoluble in most polar solvents, but sufficiently soluble in nonpolar solvents, thus allowing the easy preparation of Langmuir films simply by using pure water as a subphase.

The surface pressure vs. area (π–A) Langmuir isotherm for a floating layer of **1** on the ter subphase is reported in Figure 1. It clearly indicates the existence of two phases: the gaseous phase for pressures $\leq 1.3\ mN\,m^{-1}$ and the solid phase for $\pi \geq 4\ mN\,m^{-1}$. Moreover, it indicates that the compound can withstand pressures of up to $\pi \approx 48\ mN\,m^{-1}$, while the molecular area extrapolated to zero surface pressure is ca. 64 Å^2. This molecular area corresponds approximately to the estimated area of the hydrophilic bis(salicylaldiminato)Ni^{II} planar fragment, thus indicating that on the average the molecules lie on the surface with the dipodal hydrophobic substituents perpendicular to the surface.

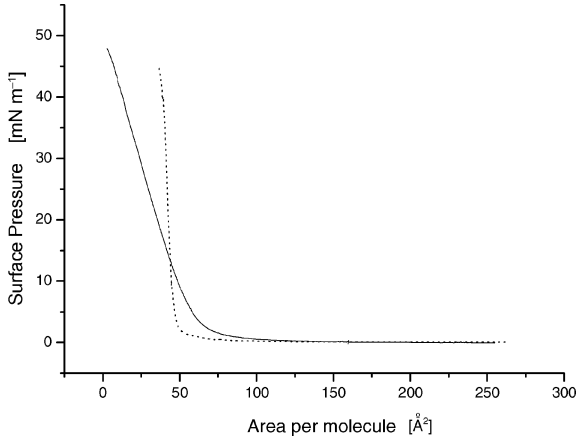

Figure 1. Surface pressure vs. area isotherms for **1** (solid) and **2** (dotted) at 293 K.

One of the most important influences on the packing of the floating films is surely the head group, as a consequence of steric hindrance as well as of its specific interactions with the molecular environment. In order to generate real and stable monolayers, a balance between hydrophobic and hydrophilic ends of the molecules is needed. In our case, strong polar groups are not present on the periphery of the Schiff base complexes, and, consequently, it is not surprising that 3D aggregates are formed on the water surface. Brewster angle microscopy (BAM) images (Figure 2), however, indicate the existence of aggregates even for low surface pressure values. The contemporaneous subsistence of three-dimensional aggregates and clean water surface is observed even just after solvent evaporation and at low surface pressures and low area densities. It is possible to distinguish a multiphase structure, with bright regions for the 3D aggregates and dark areas for the pure water surface in the image ($0.1\ mN\,m^{-1}$, Figure 2a). During compression, such domains coalesce and broaden; they begin to show more clearly facets and different shades of grey. This is illustrated in Figure 2b, taken at a surface pressure of $5\ mN\,m^{-1}$ (area per repeat unit of about 64 Å^2). Further compression at higher surface pressures permitted evidence of the generation of other clusters, even though for $\pi > 20\ mN\,m^{-1}$, the morphology of the floating film appeared not to be very sensitive to variation in the surface pressure. Such a trend is illustrated in Figure 2c and d, in which π is 20 and $47\ mN\,m^{-1}$, respectively. This behaviour is consistent with the pattern shown in the Langmuir isotherm (Figure 1), in which the slope is constantly above a pressure of $10\ mN\,m^{-1}$. Moreover, the Langmuir curve is consistent with that reported by Hemakanthi et al.[9a] for a Zn^{II} complex of a similar Schiff base, 2,4-dihydroxy-hexadecylbenzylideneamine.

The floating layers at the air–water interface were also investigated by reflection spectroscopy. In particular, the reflection of light under normal incidence at the water surface covered with a floating film of **1** was studied. This method is well suited for the investigation of the behaviour of the chromophore on the water surface, because only chromophores at the interface contribute to the enhanced reflection.[12] The difference in reflectivity (ΔR) between the floating layer of **1** on the subphase and the bare subphase was monitored as a function of the wavelength. The corresponding reflection spectra from **1** on the water surface at different fixed surface pressures after reaching equilibrium are shown in Figure 3.

A monotonic reflection enhancement upon compression, as result of the average surface density growth, accompanied by an essentially unchanged profile is observed. This finding suggests that the nature of the aggregates remains unchanged even at high surface pressures.

Such a rigid floating film is not transferable by the usual vertical dipping method, but multilayers have been fabricated by the horizontal lifting (LS) technique onto different substrates. Films of **1** (LS-**1**) were prepared following this approach: hydrophobized quartz substrates were lowered horizontally until they made contact with the floating film

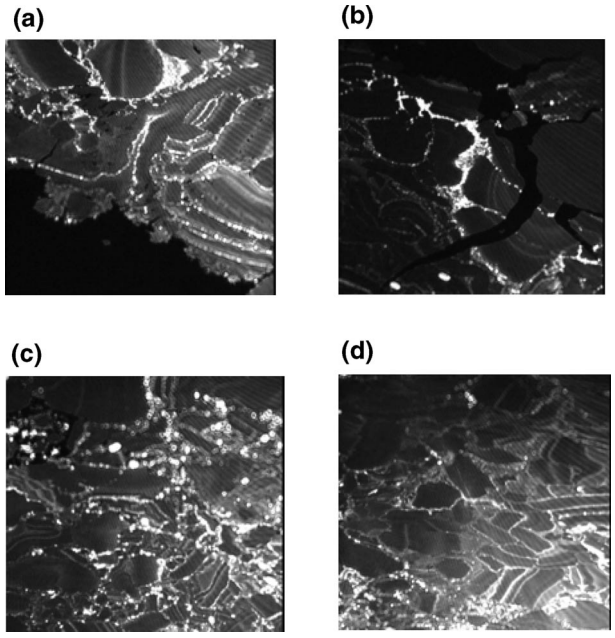

Figure 2. BAM images of the floating layer of **1** at different surface pressures: (a) 0.1 mN m^{-1}, (b) 5 mN m^{-1}, (c) 20 mN m^{-1}, (d) 47 mN m^{-1}. Width of images is 430 μm.

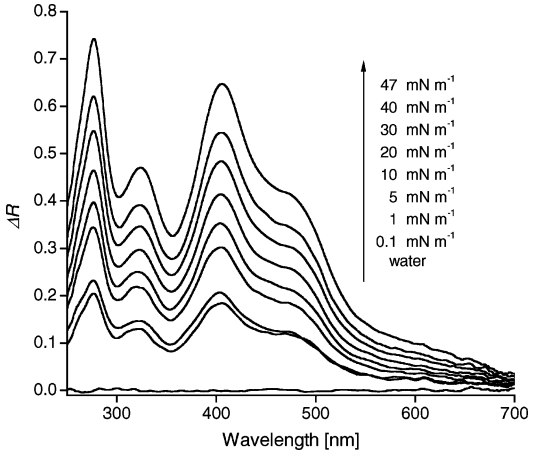

Figure 3. UV/Vis reflection spectra of **1** at the air–water interface at different surface pressures.

on the water surface. Following this procedure, a different number of runs were accomplished on the substrate at a surface pressure of 20 mN m^{-1}. The UV/Vis absorption spectra of LS-**1** for different numbers of runs are reported in Figure 4.

The absorption spectra (Figure 4) show the typical optical absorption bands for such complexes, those mainly associated with the low-energy π→π* transitions[13] at 312, 395 and 470 nm; the latter transition has a charge transfer character. The optical absorption features are fully comparable with those of complex **1** in $CHCl_3$ solution (Figure 4), with the exception of the slight redshift (≈10 nm) and increase in the intensity of the longer wavelength band. These

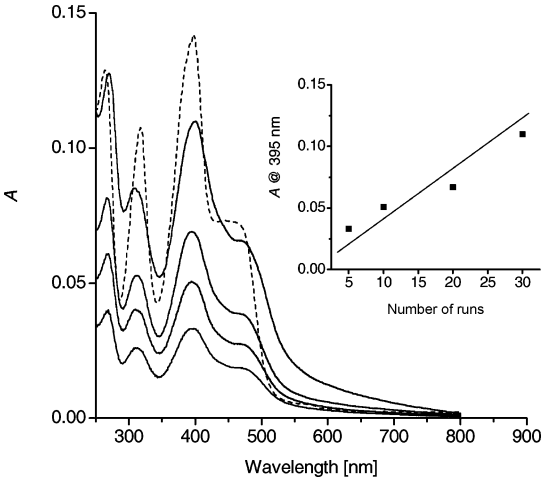

Figure 4. UV/Vis absorption spectra of LS films of **1** on quartz for different numbers of runs. The absorption spectrum of **1** in $CHCl_3$ solution (dotted) is reported for comparison. The insert shows the plot of the absorbance at 395 nm as a function of number of runs.

features are also comparable to those found for self-assembled monolayers of **1** on functionalized glass substrates.[14] In other words, even if the formation of aggregate layers occurs, it does not involve major electronic perturbation of the frontier π molecular orbitals. Moreover, the good linear relationship between the absorbance and the number of horizontal liftings (see inset Figure 4) indicates the uniformity and reproducibility of the transfer process. The overall data are thus consistent with a structure of the floating films of **1** that involves formation of aggregates (**3**) in which the planar bis(salicylaldiminato) units of each molecule presumably interact in a π–π cofacial fashion[15] in a head-to-tail configuration with respect to the molecular dipole moment (Scheme 2). Since the aromatic rings of each molecule are conjugated through the azomethinic groups,[13] such a structure will be suitable for stacking, even during the compression of the floating film.

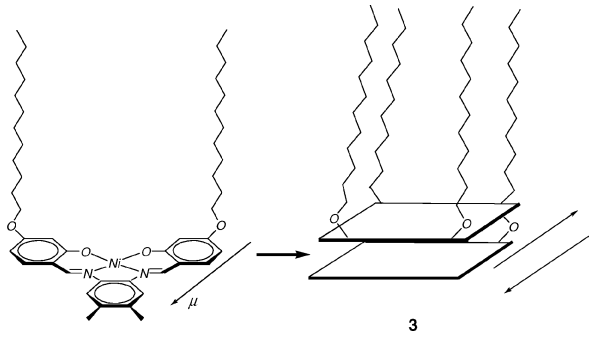

Scheme 2. Possible structure of aggregate floating layers of **1**.

Zinc(II) complexes of Schiff bases are known to exhibit a sizeable green–orange fluorescence strongly influenced by the nature of substituents on the salicylidene rings and/or on the bridging diimine.[6,16] In our case, the new alkyl-derivatized Zn^{II} species **2** was investigated. Figure 5 shows the

absorption and emission spectra of **2** in CH_2Cl_2 solution. The absorption spectrum is characterized by two bands at 315 and 372 nm and a shoulder at ca. 421 nm. The fluorescence emission is represented by an unstructured band with maximum at 510 nm, independent from the excitation wavelength. The fluorescence quantum yield, Φ_F, is ≈0.05.

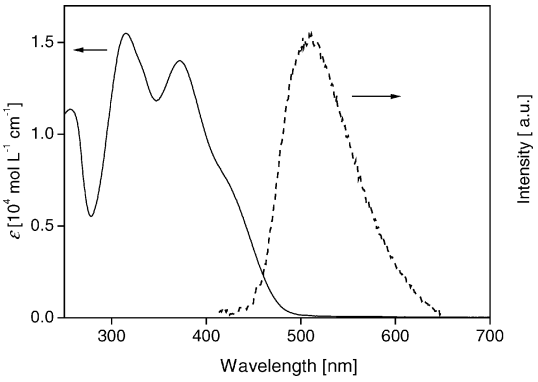

Figure 5. Absorption (solid) and fluorescence (dotted) spectra of **2** in CH_2Cl_2 solution.

Floating layers of **2**, obtained under the same experimental conditions to those of **1**, exhibits an analogous behaviour. In fact, the Langmuir isotherm indicates the formation of a solid phase for $\pi \geq 1.3$ mN m^{-1} and a molecular area extrapolated to zero surface pressure of ca. 58 Å^2 (Figure 1). The BAM images for low surface pressures indicate, analogously to **1**, the existence of 3D aggregates (Figure 6a), while for higher π values, which correspond to the solid phase, show, in contrast to **1**, the existence of a continuous and homogeneous floating film (Figure 6b).

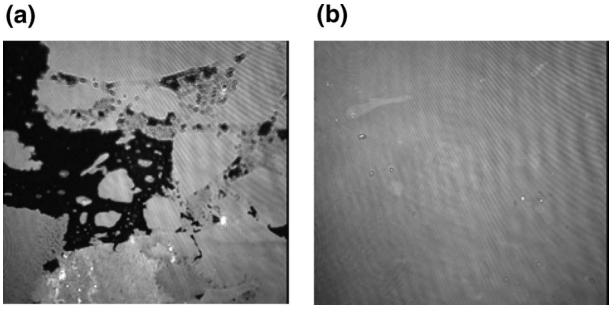

Figure 6. BAM images of the floating layer of **2** at different surface pressures: (a) 1 mN m^{-1}; (b) 15 mN m^{-1}. Width of images is 430 μm.

The UV/Vis absorption spectra of LS-**2** for different numbers of runs are reported in Figure 7. Similar to those of LS-**1**, they show the same characteristic features of absorption spectra in solution (Figure 5), with the exception of a slight redshift (ca. 8 nm) of the band at 372 nm. Moreover, the very good linear relationship between the absorbance and the number of deposited layers (see inset Fig ure 7) indicates the uniformity and reproducibility of the transfer process.

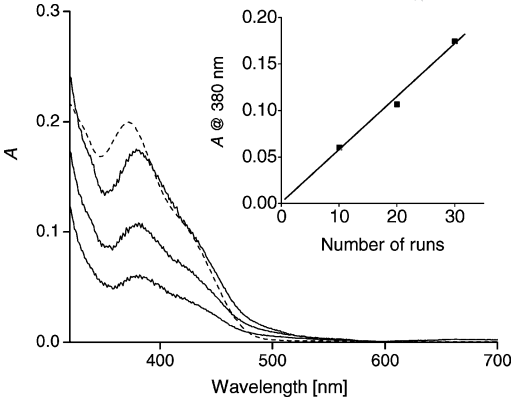

Figure 7. UV/Vis absorption spectra of LS films of **2** on glass for different numbers of runs. The absorption spectrum of **2** in CH_2Cl_2 solution (dotted) is reported for comparison. The insert shows the plot of the absorbance at 380 nm as a function of the number of runs.

Nevertheless, fluorescence measurements of these films do not show any fluorescence emission. In other words, aggregate formation, presumably as a result of π stacking of molecules through Zn···O interactions,[17] leads to a complete quenching of the fluorescence, as previously observed for analogous Zn^{II} complex aggregates[18] and for various fluorophore aggregates.[19] On the other hand, we have previously found that self-assembled monolayers of Zn^{II} complexes, analogous to **2**, possess fluorescence features (integrated emission, intensity, and emission maximum) comparable to those of the complex in solution.[20]

In order to verify the above supposition, i.e. dependence of emission on molecular environment, mixed LS multilayer films of **2** were prepared. In particular, mixed layers (1:10 molar ratio) with arachidic acid (AA) as a spacer diluent[22] were obtained (LS-**2**-AA). The Langmuir isotherm for the floating layer of **2**-AA (Figure 8) shows the existence of a solid phase for $\pi \geq 5$ mN m^{-1}, while the molecular area extrapolated to zero surface pressure is ca. 22 Å^2, which corresponds to that of arachidic acid.[3] The BAM images, independently from the surface pressure, clearly indicate the

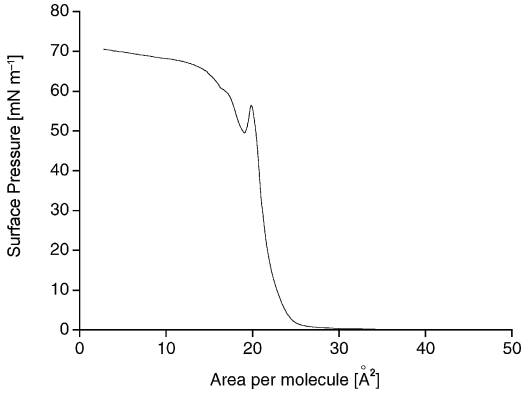

Figure 8. Surface pressure vs. area isotherm for **2**-AA (1:10) at 293 K.

existence of a homogeneous floating monolayer (Figure 9). These results suggest that at high surface pressures, the Schiff base complexes in the mixed floating film on the water surface are gradually squeezed out of the acid monolayer. The Schiff base molecules are therefore finally probably positioned in contact with the ends of the hydrocarbon lipophilic tails of the arachidic acid molecules, which result in an arachidic acid monolayer covered with Schiff base moieties. This is also consistent with the larger affinity of the Schiff base towards the hydrophobic matrix formed by the arachidic acid tails than that towards the polar water surface. The same behaviour was already suggested in other investigations on LB films of mixtures of the fatty acid and porphyrins.[21] In particular, the pattern of the Langmuir curve is very similar to that reported by Arnold.[21a]

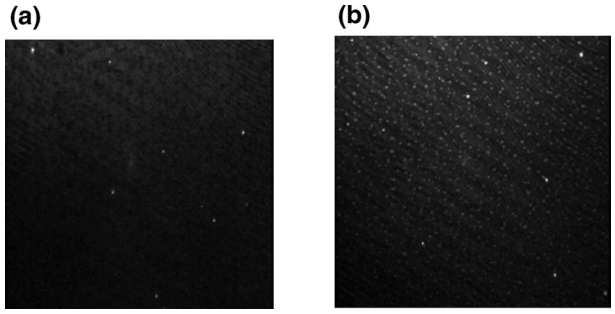

Figure 9. BAM images of the floating layer of **2**-AA at (a) 1 mN m^{-1} and (b) 23 mN m^{-1}. Width of images is 430 μm.

Optical absorption and fluorescence spectroscopy results of a representative LS-**2**-AA film are reported in Figure 10. As expected, even though the signal is noisy and has a low intensity, both absorption and fluorescence spectra are comparable to those of **2** in CH_2Cl_2 solution, as also further confirmed by fluorescence excitation spectroscopy.

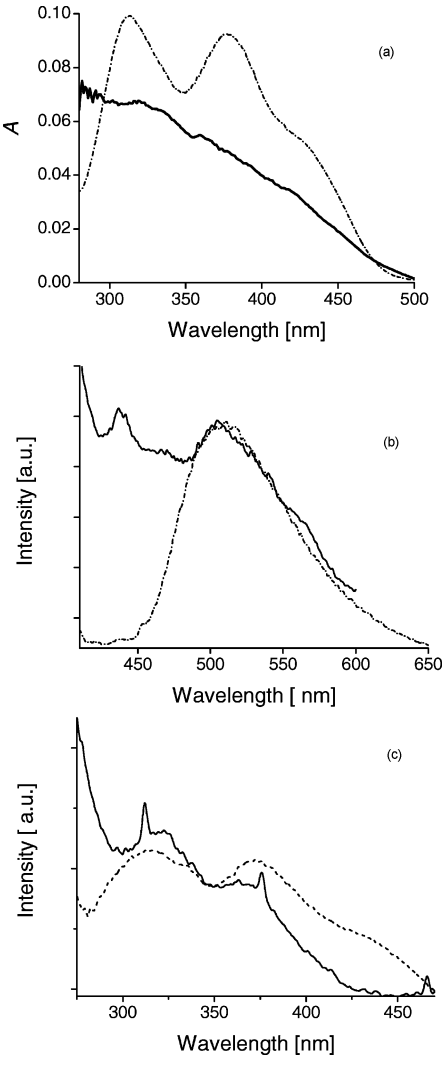

Figure 10. (a) Absorption, (b) fluorescence emission and (c) fluorescence excitation spectra of a mixed LS multilayer (100 runs) of **2**-AA on quartz. Related spectra of **2** in CH_2Cl_2 solution (dotted) are reported for comparison. The emission and excitation spectra were taken with λ_{ex} = 400 nm and λ_{em} = 500 nm, respectively.

Conclusions

In summary, the synthesis of novel functional amphiphilic Ni^{II} and Zn^{II} Schiff base complexes allowed the preparation and detailed structural and optical characterization of multilayer LS films. The existence of stacked 3D aggregates is observed for all films, even in the floating layer at low surface pressures. Aggregate formation, however, does not involve major electronic perturbation of frontier orbitals, as evidenced by the absorption spectra that are similar to those reported in solution or in self-assembled monolayers. Fluorescence emission, however, is much more sensitive to the chemical environment, and a complete quenching is observed in multilayer LS aggregates. In the limit of negligible interchromophore interactions, as in the case of mixed LS multilayers, the fluorescence is restored by using arachidic acid as a spacer diluent, and LS layers of **2** behave as related self-assembled monolayers; the latter is characterized by relatively high surface coverage.[3]

Further studies are in progress to probe the influence of hindered Schiff bases or the coordination of apical ligands on the Zn^{II} complexes[23] on the aggregation and fluorescence of the LS multilayers.

Experimental Section

Materials: Nickel(II) acetate tetrahydrate, Zinc(II) acetate dihydrate, 2,4-dihydroxybenzaldehyde, sodium *tert*-butoxide, anhydrous potassium carbonate and 1-iodododecane (Aldrich) were used without further purification. 4,5-Dichloro-1,2-phenylenediamine and 1,2-phenylenediamine (Aldrich) were purified by sublimation in vacuo.

Physical Measurements: Elemental analyses were performed on a Carlo Erba 1106 elemental analyzer. ^{1}H NMR spectra were recorded on a VARIAN INOVA 500 spectrometer, by using TMS as internal standard. Absorption spectra were recorded with a Beckman DU 650 spectrophotometer. Fluorescence spectra were recorded with a Spex Fluorolog-2 (mod. F-111) spectrofluorimeter, equipped with a double monochromator. The fluorescence quantum yield was obtained by using quinine sulfate in 1 N H_2SO_4 as

standard. The absorbance values of the solutions at the excitation wavelength were lower than 0.15 for a 1-cm pathlength. Fluorescence measurements on LS Zn^{II} multilayer films were carried out in a front face configuration, the emission was collected at an angle of 22° with respect to the excitation beam. ESI-MS were recorded on an Agilent 1100 Series ESI/MSD spectrometer. Experimental conditions were as follows: capillary voltage 3.5 KV, fragmentor 150 V, source temperature 350 °C, drying gas N_2 (10 L/min), carrier solvent methanol (0.4 mLmin^{-1}). The sample was dissolved in $CHCl_3$ containing one drop of formic acid.

Synthesis of [*N*,*N*′-Bis(4-dodecyloxy-2-hydroxybenzylidene)-4,5-dichloro-1,2-phenylenediaminato]Ni^{II} (1): In a 250-mL two-neck flask, equipped with a condenser, magnetic stirring bar and an addition funnel, an excess of 1-iodododecane (0.90 mL, 3.6 mmol) in dmf (10 mL) was placed. The solution was heated at 80 °C, and then a solution of Ni^{II}[*N*,*N*′-bis(2,4-dihydroxybenzylidene)-4,5-dichloro-1,2-phenylenediaminato]disodium salt[14] (0.233 g, 0.450 mmol) in dmf (150 mL) was added dropwise. The solution was heated at reflux overnight, then cooled and poured into methanol (300 mL), whilst stirring, to yield a red-wine solid. The solid was collected by filtration and dried under vacuum at room temperature. The solid was then adsorbed onto silica gel and chromatographed (R_f = 0.19; dichloromethane/*n*-hexane = 60/40) to yield 0.204 g (56%) as a red-orange solid (m.p. 159–162). $C_{44}H_{60}Cl_2N_2NiO_4$ (810.56): calcd. C 65.20, H 7.46, N 3.46; found C 65.90, H 7.74, N 3.69. ESI-MS: *m*/*z* (%) = 809 (87), 811 (100) $[MH]^+$. ^1H NMR (500 MHz, $CDCl_3$): δ = 0.84 (t, *J* = 6.8 Hz, 6 H, CH_3), 1.25–1.40 (m, 40 H, CH_2), 3.95 (t, *J* = 6.5 Hz, 4 H, OCH_2), 6.32 (dd, *J* = 9.0, 2.0 Hz, 2 H, Ph), 6.57 (d, *J* = 2.0 Hz, 2 H, Ph), 7.16 (d, *J* = 9.0 Hz, 2 H, Ph), 7.67 (s, 2 H, Ph), 7.87 (s, 2 H, CH=N) ppm. UV/Vis ($CHCl_3$): λ_{max} (ε, $\times 10^4$ $M^{-1}cm^{-1}$) = 317 (2.14), 398 (2.83), 460 (1.45) nm.

Synthesis of [*N*,*N*′-Bis(4-dodecyloxy-2-hydroxybenzylidene)-1,2-phenylenediaminato]Zn^{II} (2): 1-iodododecane (0.49 mL, 2.0 mmol) was added to a suspension of K_2CO_3 (0.553 g, 4.00 mmol) and Zn^{II}[*N*,*N*′-bis(2,4-dihydroxybenzylidene)-1,2-phenylenediaminato][20a] (0.412 g, 1.00 mmol) in anhydrous dmf (3 mL). The mixture was heated at 125 °C (oil-bath temperature) for 24 h, cooled to room temperature, and poured into a 10% NaOH solution (20 mL). The solid was collected by filtration, washed first with water, then with methanol, and dried in air. The brown solid was crystallized from a mixture of EtOH and $CHCl_3$ to yield 0.43 g (57%) of a brown–yellow solid (m.p. 160–162 °C dec.). $C_{44}H_{62}N_2O_4Zn$ (748.36): calcd. C 70.62, H 8.35, N 3.74; found C 70.90, H 8.50, N 3.61. ESI-MS: *m*/*z* (%) = 769 (100) $[M + Na]^+$. ^1H NMR (500 MHz, $CDCl_3$): δ = 0.89 (t, *J* = 6.9 Hz, 6 H, CH_3), 1.25–1.40 (m, 40 H, CH_2), 3.74 (t, *J* = 6.6 Hz, 4 H, $ArOCH_2$), 6.11 (m, 4 H, ArH), 6.86 (m, 2 H, ArH), 7.26 (m, 2 H, ArH), 7.36 (d, *J* = 9.0 Hz, 2 H, ArH), 8.33 (s, 2 H, CH=N) ppm. UV/Vis (CH_2Cl_2): λ_{max} (ε, $\times 10^4$ $M^{-1}cm^{-1}$) = 315 (1.55), 372 (1.40), 421 (sh.) (7.72) nm.

Langmuir Experiments – Film Preparation: Films of **1** and **2** on quartz slides (30 × 40 mm), previously hydrophobized by exposure for 24 h to a saturated atmosphere of 1,1,1,3,3,3-hexamethyldisilazane, were obtained by the Langmuir–Schäfer method (horizontal lifting) by using a KSV 5000 System 3 Langmuir–Blodgett apparatus (subphase surface of 850 cm^2). Chloroform was used to make up the spreading solutions: **1** (1.00 mg, 1.2×10^{-4} mol) and **2** (1.00 mg, 1.3×10^{-4} mol) were completely dissolved in chloroform (10 mL). Ultrapure water (resistance larger than 18 MΩcm) from a Milli-Q/Elix3 Millipore system was used as the subphase. The subphase was thermostatted at 293 K by a Haake GH-D8 apparatus. The spreading solutions (200–400 μL aliquots) were spread onto the subphase. After solvent evaporation, the floating film was compressed at a speed of 5 $Å^2$molcule^{-1}min^{-1}. In each case, the floating film was compressed without exceeding the collapse pressure and then relaxed through several cycles until reproducible curves were obtained. Usually three or four cycles were sufficient. Mixed films of **2** were also prepared by using arachidic acid as diluent in a 1:10 molar ratio; the Schiff base and arachidic acid were dissolved in chloroform.

Langmuir Experiments – Reflection Spectroscopy and Brewster Angle Microscopy: Reflection spectroscopy BAM analysis were carried out using a NIMA 601BAM apparatus, at a compression speed of 5 $Å^2$molcule^{-1}min^{-1}. The reflection data (ΔR) were obtained by an NFT RefSpec Instrument. They were acquired under normal incidence of radiation according to the description given in Ref.[12] and correspond to the difference between the reflectivities of the floating film/liquid interface and the clean air/liquid interface. All reflection spectra were obtained at 293 K. BAM measurements were carried out on an NFT BAM2*plus* system with a lateral resolution of 2 μm.

Acknowledgments

We gratefully thank the Ministero dell'Istruzione, dell'Università e della Ricerca (MIUR, Italy, PRIN 2006, n. 2006034018 and n. 20066031909) for financial support.

[1] M. Petty in *Molecular Electronics*, Wiley-VCH, Weinheim, **2007**.
[2] J. P. Dakin, R. G. W. Brown in *Handbook of Optoelectronics*, CRC, Boca Raton, **2006**, vols. 1, 2.
[3] See, for example: D. Möbius, R. Miller (Eds.), *Organized Monolayers and Assemblies: Structure, Processes, and Function*, Elsevier, Amsterdam, **2002**; A. Ulman, *Chem. Rev.* **1996**, *96*, 1533–1554; A. Ulman in *An Introduction to Ultrathin Organic Films: From Langmuir–Blodgett to Self-Assembly*, Academic Press, New York, **1991**.
[4] L. Torsi, G. M. Farinola, F. Marinelli, M. C. Tanese, O. Hassan Omar, L. Valli, F. Babudri, F. Palmisano, P. G. Zambonin, F. Naso, *Nat. Mater.* **2008**, *7*, 412–417.
[5] P. G. Cozzi, *Chem. Soc. Rev.* **2004**, *33*, 410–421.
[6] a) H.-C. Lin, C.-C. Huang, C.-H. Shi, Y.-H. Liao, C.-G. Chen, Y.-C. Lin, Y.-H. Liu, *Dalton Trans.* **2007**, 781–791; b) P. G. Cozzi, L. S. Dolci, A. Garelli, M. Montalti, L. Prodi, N. Zaccheroni, *New J. Chem.* **2003**, *27*, 692–697.
[7] a) S. Di Bella, *Chem. Soc. Rev.* **2001**, *30*, 355–366; b) P. G. Lacroix, *Eur. J. Inorg. Chem.* **2001**, 339–348; c) O. Margeat, P. G. Lacroix, J. P. Costes, B. Donnadieu, C. Lepetit, K. Nakatani, *Inorg. Chem.* **2004**, *43*, 4743–4750.
[8] a) J. Nagel, U. Oertel, P. Friedel, H. Komber, D. Möbius, *Langmuir* **1997**, *13*, 4693–4698; b) S. Shyamala Sundari, A. Dhathathreyan, M. Kanthimathi, B. U. Nair, *Langmuir* **1997**, *13*, 4923–4925.
[9] a) G. Hemakanthi, A. Dhathathreyan, D. Möbius, *Colloid Surf. A* **2002**, *198–200*, 443–452; b) G. Hemakanthi, B. U. Nair, A. Dhathathreyan, *Chem. Phys. Lett.* **2001**, *341*, 407–411; c) H. Abe, K. Miyamura, *Inorg. Chim. Acta* **2000**, *298*, 90–93.
[10] a) P. Guo, M. Liu, *Langmuir* **2005**, *21*, 3410–3412; b) P. Guo, M. Liu, *Colloid Surf. A* **2006**, *284–285*, 70–73.
[11] H. Nakahara, K. Fukuda, D. Möbius, H. Kuhn, *J. Phys. Chem.* **1986**, *90*, 6144–6148.
[12] H. Kuhn, D. Möbius, "Monolayer Assemblies" in *Physical Methods of Chemistry, Vol. IXB. Investigations of Surfaces and Interfaces – Part B* (Eds: B. W. Rossiter, R. C. Baetzold), Wiley-Interscience, New York, **1993**, p. 375.
[13] S. Di Bella, I. Fragalà, I. Ledoux, M. A. Diaz-Garcia, T. J. Marks, *J. Am. Chem. Soc.* **1997**, *119*, 9550–9557.

[14] S. Di Bella, I. Fragalà, N. Leonardi, S. Sortino, *Inorg. Chim. Acta* **2004**, *357*, 3865–3870.
[15] K. Miyamura, A. Mihara, T. Fujii, Y. Gohshi, Y. Ishii, *J. Am. Chem. Soc.* **1995**, *117*, 2377–2378.
[16] a) M. La Deda, M. Ghedini, I. Aiello, A. Grisolia, *Chem. Lett.* **2004**, *33*, 1060–1061; b) P. Wang, Z. Hong, Z. Xie, S. Tong, O. Wong, C.-S. Lee, N. Wong, L. Hung, S. Lee, *Chem. Commun.* **2003**, 1664–1665.
[17] a) J. K.-H. Hui, Z. Yu, M. J. MacLachlan, *Angew. Chem. Int. Ed.* **2007**, *46*, 7980–7983; b) A. W. Kleij, M. Kuil, M. Lutz, D. M. Tooke, A. L. Speck, P. C. J. Kamer, P. W. N. M. van Leeuwen, J. N. H. Reek, *Inorg. Chim. Acta* **2006**, *359*, 1807–1814.
[18] C. T. L. Ma, M. J. MacLachlan, *Angew. Chem. Int. Ed.* **2005**, *44*, 4178–4182.
[19] See, for example: a) H. Kobayashi, M. Sasaki, N. Ohsawa, K. Yasuda, M. Kotani, *J. Phys. Chem. C* **2007**, *111*, 268–271; b) M. Kawasaki, S. Aoyama, E. Kozawa, *J. Phys. Chem. B* **2006**, *110*, 24480–24485.
[20] a) S. Di Bella, N. Leonardi, G. Consiglio, S. Sortino, I. Fragalà, *Eur. J. Inorg. Chem.* **2004**, 4561–4565; b) S. Di Bella, G. Consiglio, G. La Spina, C. Oliva, A. Cricenti, *J. Chem. Phys.* **2008**, 129, 1144704-1–1144704-5.
[21] a) D. P. Arnold, D. Manno, G. Micocci, A. Serra, A. Tepore, L. Valli, *Langmuir* **1997**, *13*, 5951–5956; b) P. Lesieur, M. Vandevyver, A. Ruaudel-Teixier, A. Barraud, *Thin Solid Films* **1988**, *159*, 315–322; c) D. Möbius, M. Orrit, H. Grüniger, H. Meyer, *Thin Solid Films* **1985**, *132*, 41–53.
[22] This ratio represents the best value in order to observe the maximum fluorescence efficiency.
[23] See, for example: E. C. Escudero-Adán, J. Benet-Buchholz, A. W. Kleij, *Inorg. Chem.* **2008**, *47*, 410–412.

Received: July 24, 2008
Published Online: October 16, 2008

